DIGITAL 3D MAPPING OF ACTIVE FAULTS BENEATH SANTA MONICA BAY, BASIN MODELING, AND STRAIN PARTITIONING: COLLABORATIVE RESEARCH UCSB AND LDEO

USDI/USGS 03HQGR0048 (UCSB)
USDI/USGS 03HQGR0005 (Columbia)

Principle Investigators: Christopher C. Sorlien
Institute for Crustal Studies, University of California, Santa Barbara, California, 93106
Leonardo Seeber, Lamont-Doherty Earth Observatory, Columbia University, Palisades, New York 10964
ICS Telephone (805)-893-8231, ICS FAX (805)-893-8649
Sorlien email: chris@crustal.ucsb.edu
Sorlien URL: www.crustal.ucsb.edu/~chris
Co-authors on the project: Kris Broderick, UCSB; Ray Sliter, USGS; Bill Normark, USGS; Mike Fisher, USGS; Marc Kamerling, Venoco Inc; Bruce Luyendyk, UCSB

NEHRP Element: I Keywords: Neotectonics, Reflection Seismology; Tectonic Structures, Fault Segmentation

Research supported by the U.S. Geological Survey (USGS), Department of the Interior, under USGS award number USDI/USGS 03HQGR0048. The views and conclusions contained in this document are those of the authors and should not be interpreted as necessarily representing the official policies, either expressed or implied, of the U.S. Government

INVESTIGATIONS UNDERTAKEN

We used industry and USGS seismic reflection data controlled by well and seafloor data to map blind faults and also several other faults that reach to or close to the seafloor. This work covers the area south of the mainland coast from Palos Verdes Hills through the Malibu Coast to Port Hueneme, which we loosely call northern Santa Monica Bay (**Fig. 1**). The maps were constructed digitally, depth-converted, and provided to the SCEC Community Fault Model (**Fig. 2**). In addition to these fault maps and our previously mapped lower Pliocene horizon, digital maps on base Pliocene and of the late Pliocene top "Repetto" horizon have been completed over the whole area. A ~50 ka horizon is correlated from ODP site 1015 (Normark and McGann, 2003; Shipboard Scientific Party, 1997) through part of the study area. This stratigraphic control allowed changes in deformation through time to be studied. Simple modeling of dip-slip on blind faults was performed on cross sections. Details of the Santa Monica-Dume faults system and modeled slip on this fault system is discussed in our previous Final Technical Report (Sorlien et al., 2003). New mapping and stratigraphic correlation provides more information on connections between these faults and on subsidence of the footwall basin. Here, we focus on blind and seafloor faults farther south.

INTRODUCTION

Several destructive earthquakes that affected metropolitan Los Angeles have occurred on blind faults. Blind faults have been inferred in and around Los Angeles in order to explain folding of the shallow crust. The largest anticlinoria along the southern California margin and Borderland, including the one expressed as the Santa Monica Mountains and Northern Channel Islands, can extend 200 km along trend and 50 km across trend (Shaw and Suppe, 1994; Davis and Namson, 1994a, b; Seeber and Sorlien, 2000). Very large anticlinoria are associated with a blind component of slip on faults of equal or larger size. Blind thrusts have been imaged on seismic reflection data, one example being the Puente Hills thrust beneath northeast Los Angeles basin (Shaw and Shearer, 1999). The southwest margin of Los Angeles basin has been interpreted as a backlimb above a NE-dipping blind thrust ramp called the Compton-Los Alamitos thrust (Shaw and Suppe, 1996; see also Davis et al., 1989). While proposed slip rates on this fault are low (1.4 +/- 0.4 mm/yr; Shaw and Suppe, 1996), and its existence is controversial, recent earthquakes in southern California suggest that a failure on one or more of its segments would be devastating.

The Palos Verdes Hills are the surface expression of a NW-trending anticlinorium (Dibblee, 1999). The southwest limb of this fold was explained as a backlimb above a SW-dipping backthrust that forms the roof of a SW-directed tectonic wedge (Davis et al., 1989; Shaw and Suppe, 1996). The tip of this wedge is located beneath the deep San Pedro Basin in the interpretation of Davis et al. (1989). In this interpretation, the SW-dipping backthrust explains the entire SW-dipping limb that extends from Palos Verdes hills offshore beneath the San Pedro escarpment (**Fig. 3A**). Alternatively, the tip of the southwest-directed wedge is near the coastline does not explain the San Pedro escarpment in the interpretation of Shaw and Suppe (1996). Finally, it is possible to dispense with the backthrust altogether and still explain the entire onshore-offshore fold limb. Within our study area, we interpret the San Pedro escarpment to be a broad forelimb above a NE-dipping fault or fault system.

Structural highs extend offshore to the southeast and northwest of Palos Verdes Hills. The northwest extension has been called the Shelf Projection (**Figs. 3A,3B**; e.g., Nardin and Henyey,

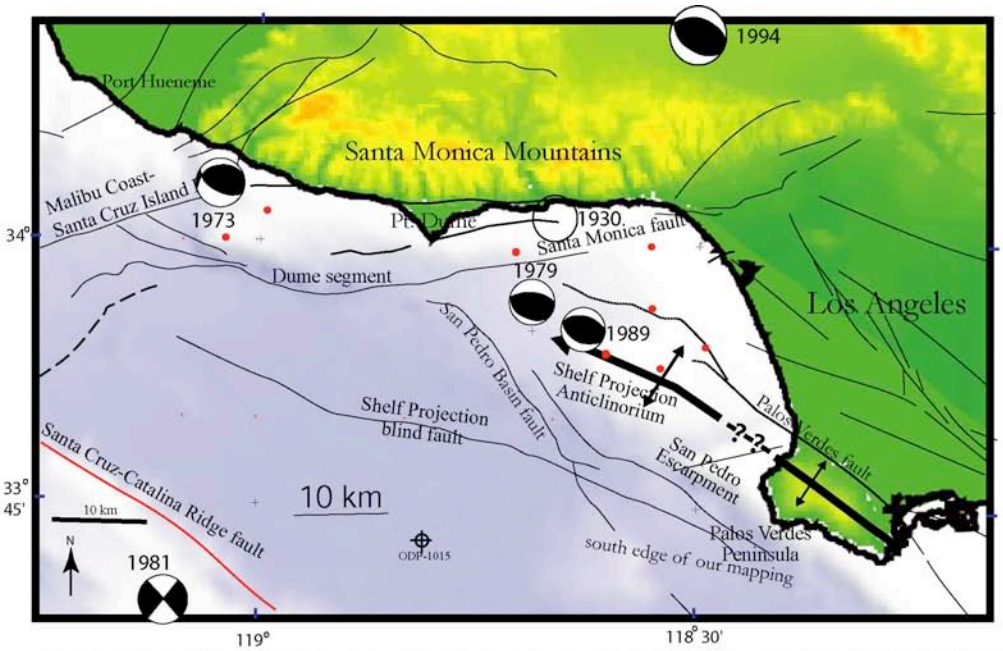

Figure 1: Fault map of Santa Monica Bay and vicinity. Focal mechanisms from USGS and SCEC (1994) and Haukkson and Saldivar (1986). Red dots are those wells used in the project (others exist). The Palos Verdes anticlinorium extends WNW beneath the Shelf Projection.

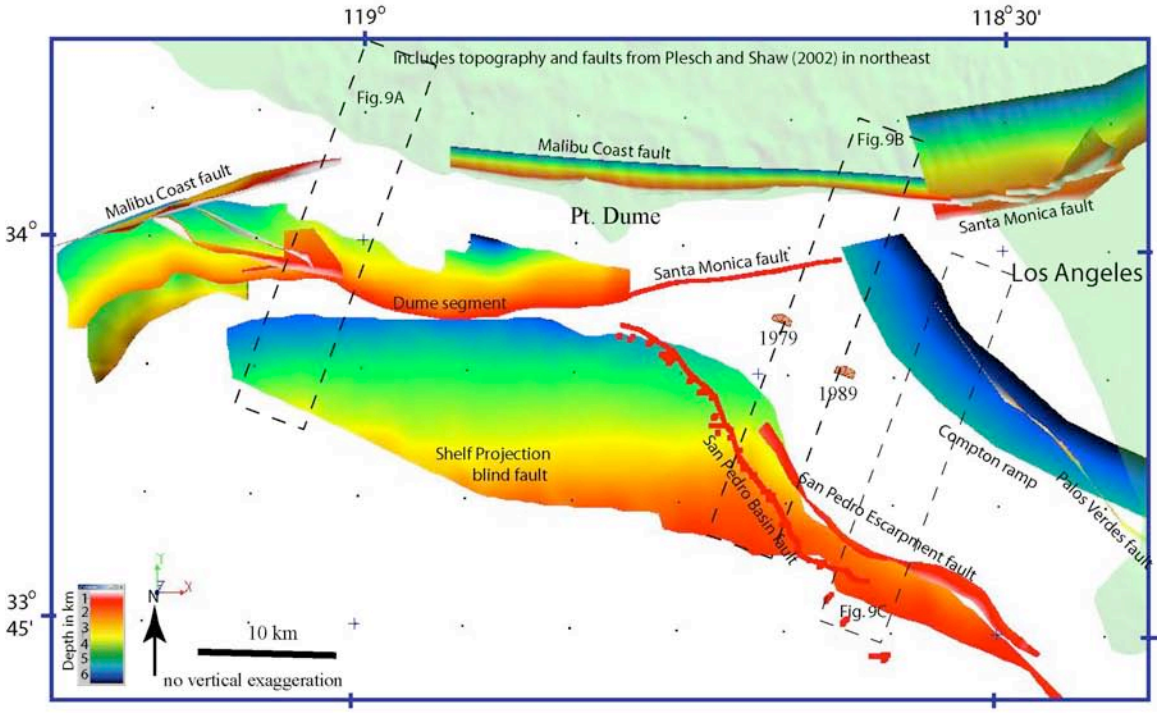

Figure 2: Map of fault surfaces. The onshore Malibu Coast fault, onshore Santa Monica Fault, Compton ramp, and Palos Verdes fault are from Plesch and Shaw (2002) and are made transparent below 6.5 km. The other faults were supplied by us to the SCEC CFM. The Southeast part of our Shelf Projection blind fault and the San Pedro escarpment fault are aligned in 3D with the Compton ramp. The offshore Santa Monica fault east of Point Dume dips moderately north; we did not map it to the coast due to a data gap.

1978) or Santa Monica Plateau (Gardner et al., 2003). The Shelf Projection is the bathymetric expression of the Shelf Projection anticlinorium (**Fig. 4**; Nardin and Henyey, 1978). This anticlinorium was interpreted to be en-echelon, right-stepping with the Palos Verdes anticlinorium and offshore folds farther southeast (Nardin and Henyey, 1978). Active folding of the Shelf Projection was interpreted to pre-date 1 Ma (Nardin and Henyey, 1978), but there has been much seismicity beneath the Shelf Projection, including M5.0 earthquakes in 1979 and 1989 (**Fig. 1**; Hauksson and Saldivar, 1986; Hauksson, 1990). We re-evaluate continuity of the anticlinoria, examine evidence for active folding, map the upper parts of underlying faults, and model long-term average slip rates and how these might relate to modern slip rates.

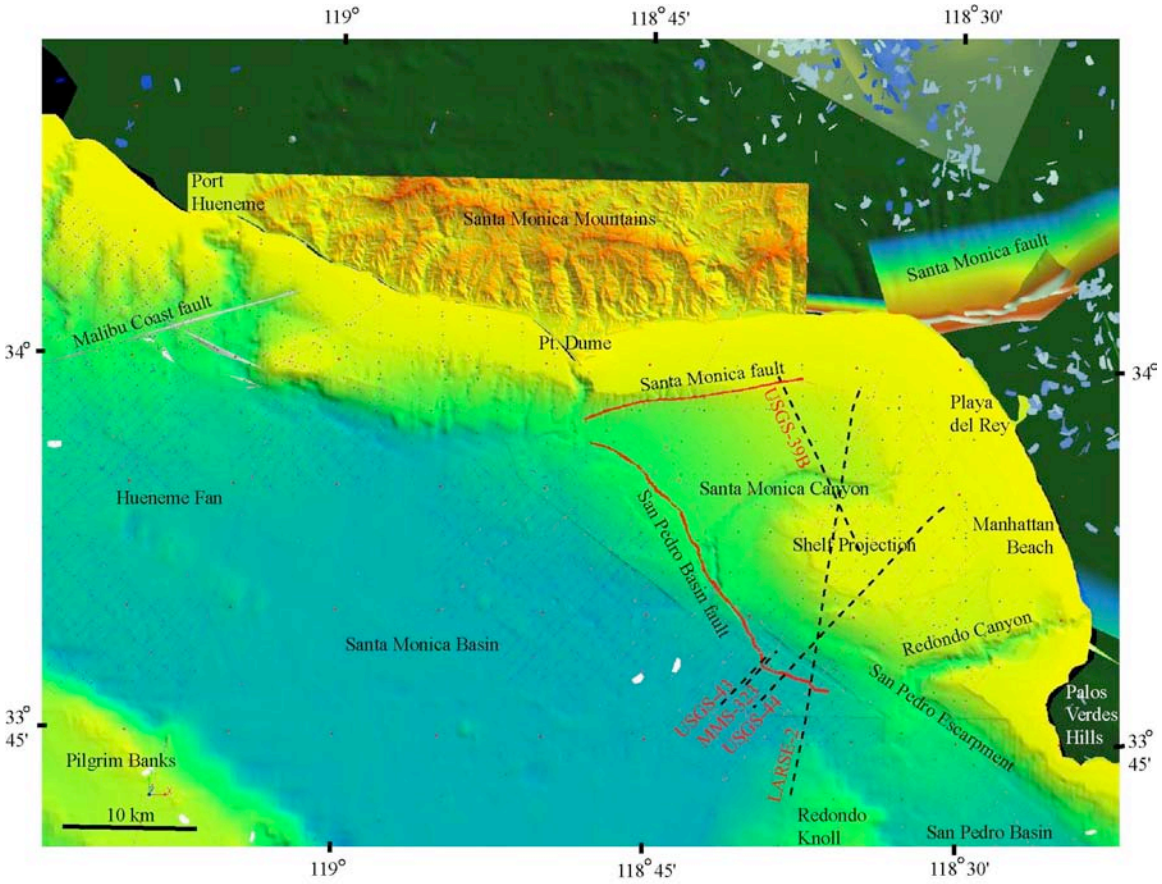

Fig. 3A: 3A-vertical view of bathymetry with no vertical exaggeration, a few seafloor faults from our mapping, and onshore faults from the SCEC CFM (Plesch and Shaw, 2002). Selected earthquake slip planes are shown through semi-transparent topography (Hauksson, 2000); part of the Santa Monica Mountains are shown as high-resolution and opaque. Faint grids of lines are part of the seismic reflection database that was used; profiles shown as labeled black dashed lines are the figures.

DATA, METHODS, AND MAPPING

Seismic Reflection Data

We used three different overlapping grids of industry multichannel seismic reflection data, and a few profiles from two other data sets to map structure in 3D and correlate stratigraphy through northern Santa Monica Bay (**Fig. 3A**, **Fig. 4 inset**). An additional 800 m x 2500 m grid of single-

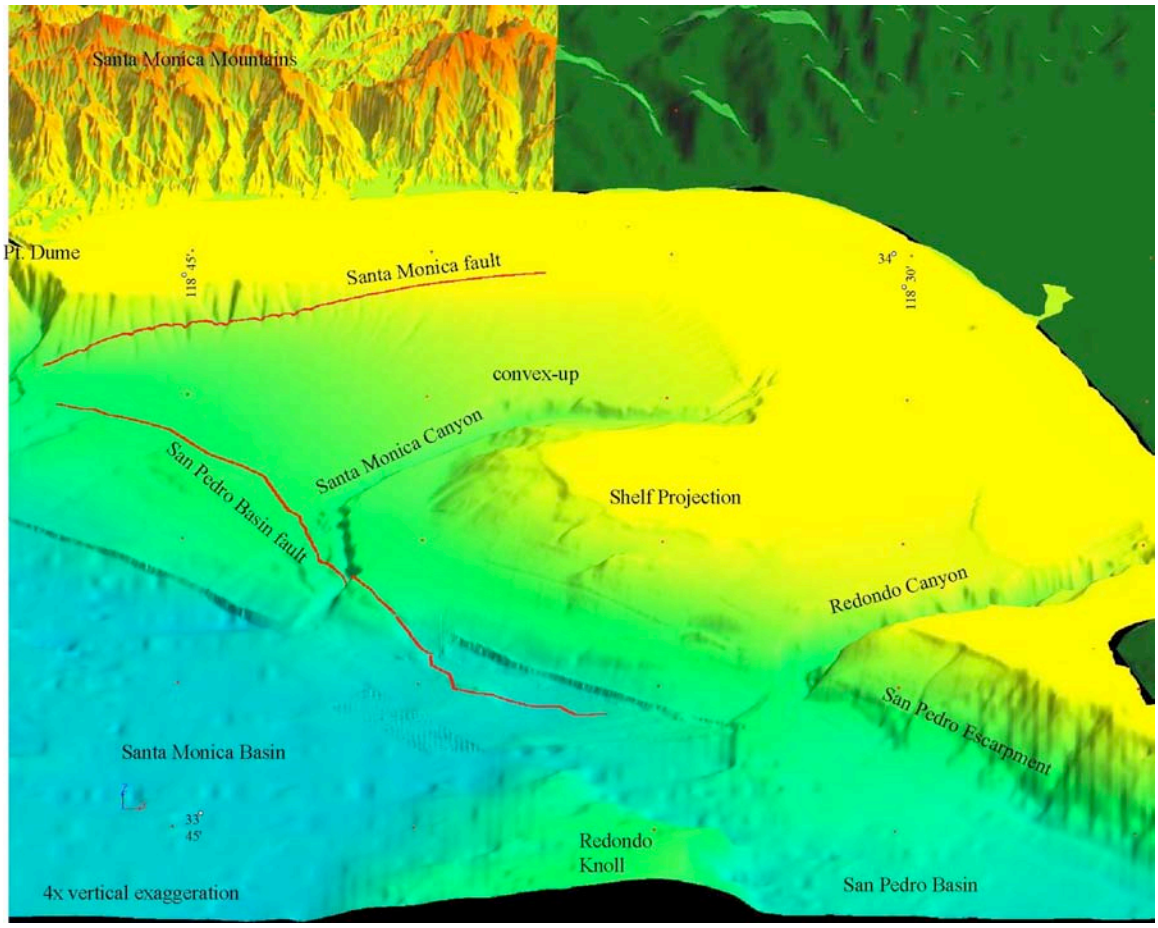

Figure 3B: Oblique view of bathymetry and topography at 4x vertical exaggeration. The sea floor trace of the Santa Monica fault was mapped using seismic reflection profiles; it coincides with disruptions of ravines. The area labeled "convex up" may be a northwest continuation of the Palos Verdes-Shelf Projection anticlinorium (see Gardner et al. 2003, for high-resolution bathymetric figures and cross sections). Santa Monica Canyon is more deeply entrenched in the "convex-up" area and near the San Pedro Basin fault.

channel sparker and minisparker reflection data was used to map part of the San Pedro Basin fault trace at the seafloor, and to correlate ODP-1015 stratigraphy (data described in Burdick and Richmond, 1982). Several multichannel profiles acquired by the USGS in 1998 and 1999 were redisplayed and four others were reprocessed (**Fig. 5**, Fisher et al., 2003; Bohannon et al., submitted). We interpreted most of the other 1998 and 1999 profiles at Menlo Park using an interactive system, with correlations made between these USGS profiles using paper prints of industry data.

Digital Mapping

The output data points from our mapping at USGS were provided as UTM-X-Y two-way travel time text files. These data were combined with data points from our interpretation of industry and MMS data, gridded, and then depth converted. This approach was used for the San Pedro Basin fault and all horizons and faults to its east, while elsewhere we digitized points from maps derived from paper prints of industry data. Digital gridded travel-time maps were converted to depth using 2 and 3 layered velocity models for the Pliocene horizon and the fault maps,

respectively (water, velocity gradient 1 above map horizon, velocity gradient 2 below map horizon). Slopes of velocity gradients were calculated from sonic logs from wells, and from stacking velocities of sub-horizontal reflections used in processing the seismic reflection data. Spatially-variable velocity slopes were used west of the San Pedro Basin fault and a constant slope was used east of that fault.

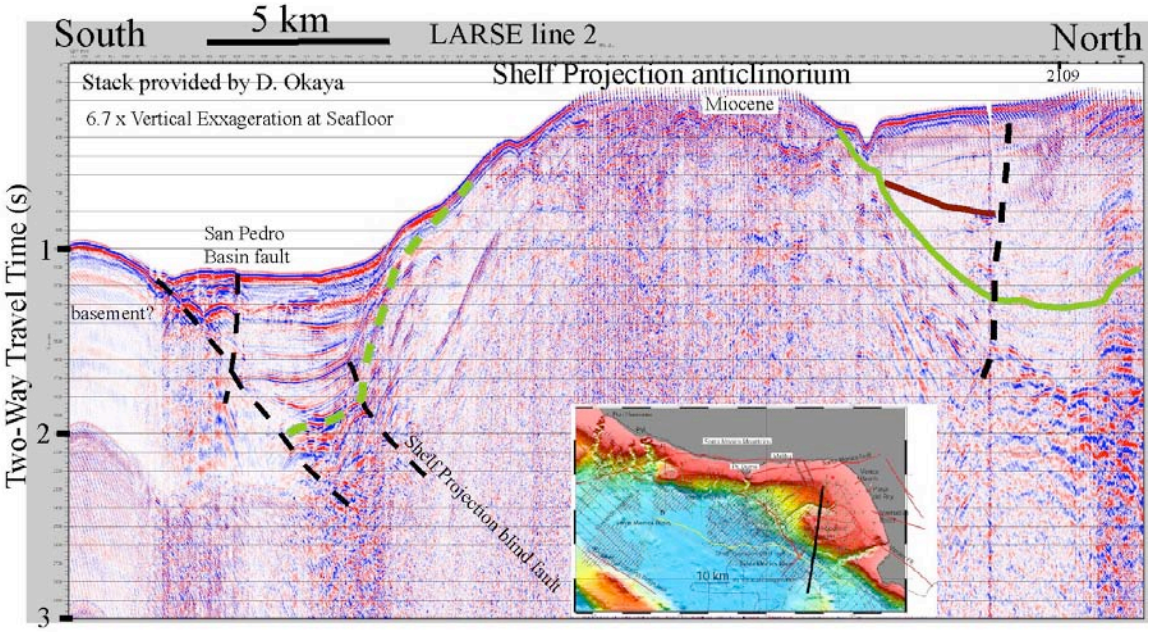

Figure 4: A stack of LARSE2, showing the anticlinorium, approximate top Miocene (green), top "Repetto" (brown), and NE-dipping Miocene normal-separation fault with probable Catalina schist in the footwall at Redondo Knoll (south end). San Pedro Escarpment fault not interpreted on this profile due to low resolution.

Seismic Processing

Several profiles were reprocessed at UCSB: USGS39B, 44, 48, and 103. The end result was not a migrated profile that was "better" than USGS processing; instead, we applied a special, somewhat radical approach to remove multiples. This involved a partial normal moveout (NMO) correction on shot gathers, FK-filtering of under-corrected reflections, and removal of the NMO correction. This was effective in removing multiples for profiles that were shot up the slope (towards the north or northeast) because the dip causes a delay for reflections to get to the far traces, in shot gathers. In the presence of dip in the opposite direction of ship travel, the apex of the hyperbolas is shifted ahead of the profile so that a more linear multiple reflection is recorded, making it susceptible to removal by FK filter (Mladen Nedimovic, oral communication, 2003). However, primary reflections with more than gentle south or southwest dips were also removed. None-the-less, in combination with standard processing, this approach allowed interpretation beneath the water bottom multiple, despite the short (250 m) streamer **(Fig. 5)**. A Finite Difference migration, output in depth and travel time, was applied to two profiles. A velocity model in layers, using realistic interval velocities from our experience in the region, was used for the depth migration, and for a time-to-depth conversion of an additional profile.

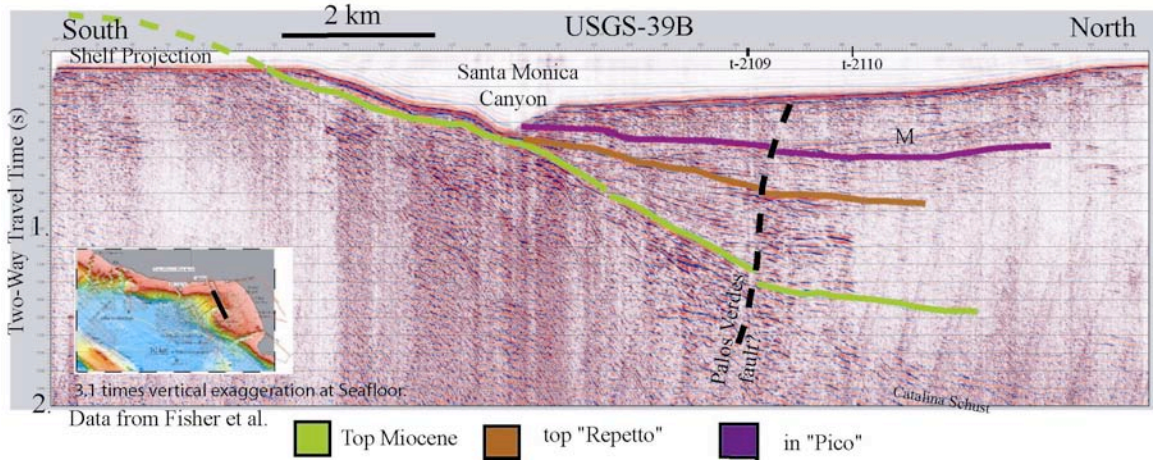

Figure 5: Our specially-processed stack across the north limb of the Palos Verde-Shelf Projection anticlinorium, where S-dipping multiples ("M"), and some steeper S-dipping primaries were removed, so that the progressive tilting of the strata is imaged. Located by the heavy black line in the inset and on Fig. 3A.

Stratigraphy and digital maps

Stratigraphic control was provided by logs from several wells drilled in the hanging-wall of the Dume fault, including 2 with sonic logs (**Fig. 2**). The well information was converted to travel time and correlated through the grids of reflection data, and around the east and west plunge of the Dume fault into the footwall basin to the south. Stratigraphic and paleontologic information from two wells constrain the interpretation in the basin between the Santa Monica fault and the Shelf Projection (**Fig. 5**). This correlation was supplemented by published information on seafloor outcrop (Vedder, 1990; Nardin and Henyey, 1978), by wells on the Shelf Projection, and by stratigraphic and velocity information from coastal and offshore oil fields at Playa del Rey and Venice Beach (Cal Div. Oil and Gas, 1992, Wright, 1991). Detailed stratigraphic information is also available in that area in a technical report (Davis and Namson, 2000). Finally, stratigraphic information for the last estimated 50 ka is available from ODP site 1015 (Shipboard Scientific Party, 1997; Normark and McGann, 2003). A reflection near the base of that hole, 150 m or 200 milliseconds (ms) two-way travel time (TWTT) below seafloor (bsf), has been correlated along several paths to the San Pedro Basin fault, to the southwest limb of the Palos Verdes-Shelf Projection anticlinorium, and across the San Pedro Escarpment fault (**Figs. 6, 7**).

We previously produced structure-contour maps for 36 km along strike of the Dume segment of the Santa Monica-Dume fault, and for 50 km along strike of a blind fault beneath and south of the Santa Monica-Dume fault (Sorlien et al., 2003a). We also mapped a horizon within the lower part of the Repetto rocks which was deposited before initiation of contractile folding, and which remains distinct from time-transgressive unconformities at the base and top Repetto interval over much of the area. This horizon does, however, locally onlap strata beneath, especially in the area south and east of Pt. Dume. We estimate that its age falls within the range for the base Repetto unconformity (between 4.42 +/- 0.57 m.y. and 3.4 +/- 0.3 m.y.; Blake, 1991). During the current project, we mapped additional faults, re-mapped the blind fault, and mapped the base Pliocene and top "Repetto" (~2.5 Ma, Blake, 1991) horizons. New fault maps include the offshore Malibu Coast fault, faults strands that connect the Dume segment to the Malibu Coast fault, a seafloor trace of the Santa Monica-Dume fault east of Point Dume (**Fig. 3b**), the San Pedro Basin fault

(as 4 strands), and the southwestern strand of the San Pedro escarpment fault zone (**Fig. 2**). We also examined the offshore Palos Verdes fault, but decided that special reprocessing of the USGS data would be required to make sense of possibly several small strands (**Fig. 5**).

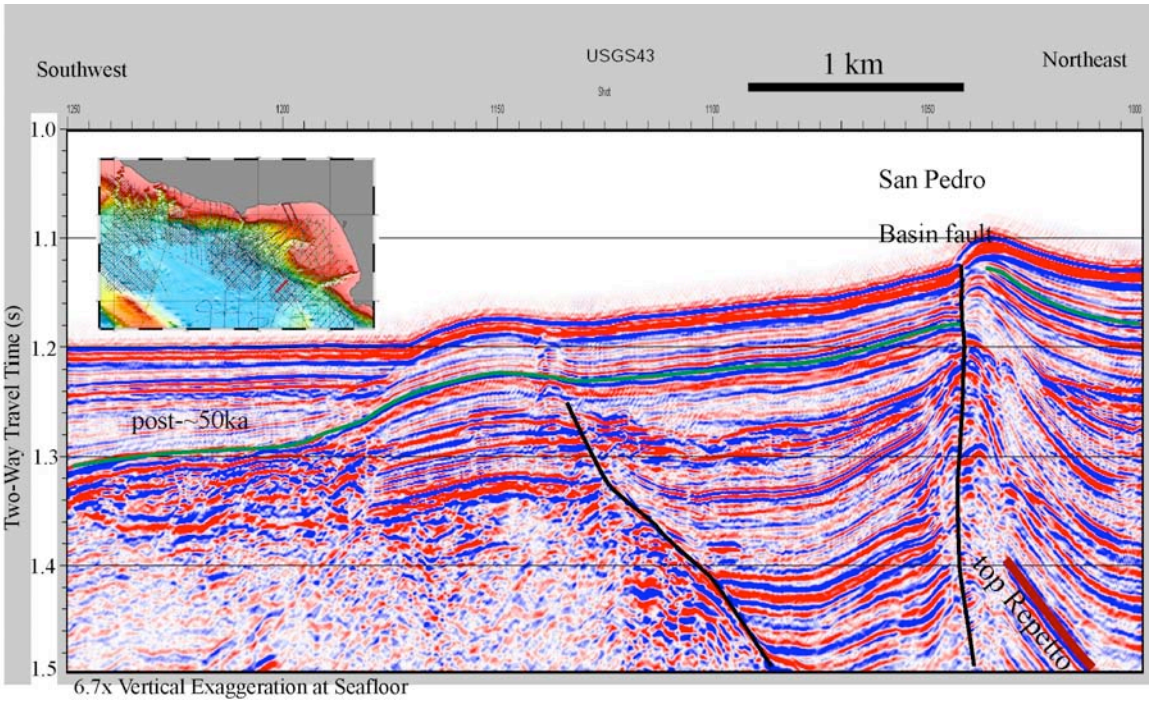

Figure 6: Migrated multichannel stack across a NE-dipping normal-separation fault, and the right-lateral San Pedro Basin fault. Located by heavy red line in inset and on Fig. 3A. The dark green horizon is the base of strata drilled at ODP site 1015. The top "Repetto" horizon is shown in brown. The reflective section below the post-50 ka strata at the southwest side may be Miocene or Pliocene.

Bathymetry and Three Dimensional Visualization

Having many different types of maps and data in the same 3D visualization system allows relationships between fault, folds, bathymetry, and seismicity to be evaluated. A digital database of geographically-registered 3D surfaces and objects was constructed using the software GOCAD (Mallett, 1992, 1997). This data base includes all of our maps of faults and stratigraphic horizons, trackline navigation of the seismic reflection data, 30 m digital elevation model (DEM) of the Santa Monica Mountains, lower resolution DEM from the SCEC Community Fault Model (CFM), faults from the CFM (Plesch and Shaw, 2002), seismicity, and bathymetry. Multibeam bathymetry, gridded at 16 m, are available for much of the study area east of Pt. Dume (Dartnell and Gardner, 1999). Eight meter resolution data in shallow areas were provided by P. Dartnell. In addition, we gridded NOAA point data for areas not covered by swath bathymetry, and combined this grid with the multibeam data, regridded at 60 m (shown in **Fig. 3**). **Figure 3b** shows that the seafloor trace of the Santa Monica fault coincides with disruptions of submarine ravines, and Santa Monica Canyon is more deeply entrenched near active faults and folds.

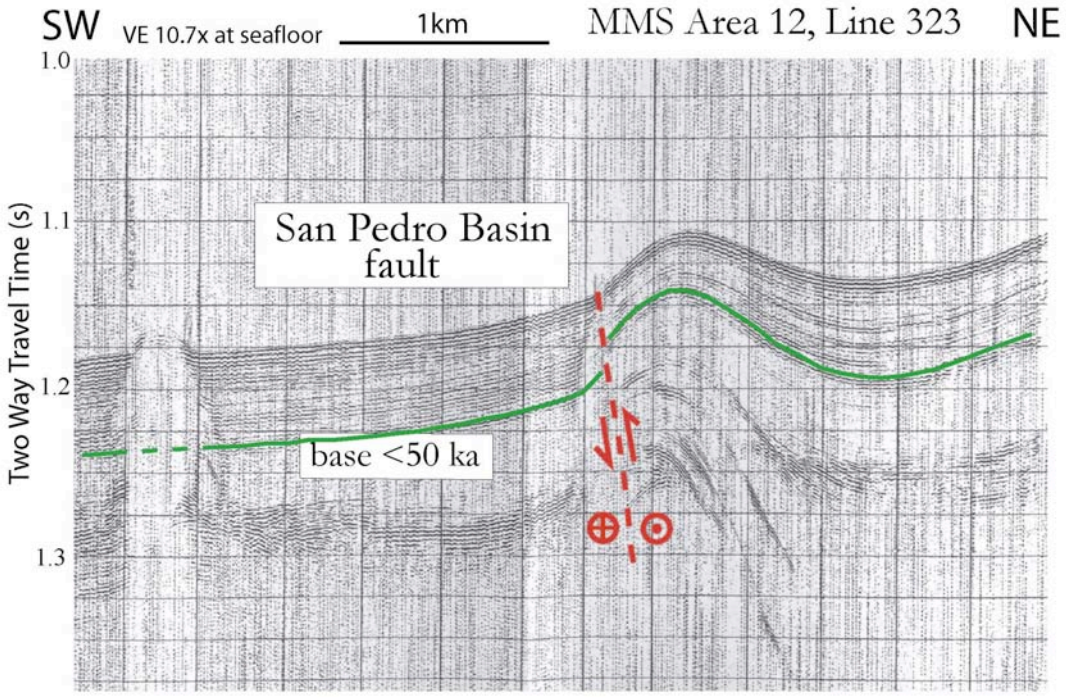

Figure 7: Minisparker profile MMS-323, located in Figure 3A, adjacent to USGS-43 (Fig. 6). Forty meters of relief since 50 ka is due to faulting, folding, and drape.

Seismicity

We previously created programs to convert precisely-relocated earthquake focal mechanisms (J. Armbruster) to GOCAD format, and imported 4714 of these for the Santa Monica-Los Angeles-San Fernando areas. For this project, we created an additional program to convert a standard earthquake format used by Hauksson (2000) to GOCAD format. For figures shown in this report, the Hauksson data are shown for years 1976 and 1981-2002, with the J. Armbruster and L. Seeber data for 1971, and for 1977-1980. Nodal planes are shown as polygons, and the slips as 3-D vectors (**Fig. 8**). The selected nodal plane and the slip of each side of each nodal plane can be displayed separately. Ten properties, including strike, dip, rake, and time, are included with each earthquake and the visualization can be limited to different ranges of these properties. The Armbruster-Seeber data have preferred nodal planes displayed, but the presumed arbitrary nodal plane is displayed for the Hauksson data.

INTERPRETATIONS

Faults

A blind N-dipping low-angle fault, the Shelf Projection blind fault, was re-mapped beneath central and eastern Santa Monica Bay, along 65 km of its strike (**Fig. 2**). We interpret it to be a basal Miocene detachment associated with clockwise vertical-axis rotation of the Santa Monica Mountains (see Kamerling and Luyendyk, 1979). It is located south of and beneath the Santa Monica-Dume fault (**Fig. 9a**). Several contractional structures indicate that it has been reactivated, with different structural styles for each. The western part, south and southwest of Pt. Dume, has been only slightly reactivated near its upper tip by post-Miocene folding. However,

its downdip projection merges with or intersects the moderately-dipping Santa Monica-Dume fault. The central and southeast part of the fault projects beneath the WNW-trending Palos Verdes anticlinorium, including a 20 km-long offshore part beneath the Shelf Projection (**Figs. 1, 9b,c**). The post-Pliocene strata above the upper part of the fault, southwest of the San Pedro escarpment, exhibit little deformation (**Fig. 10).** Thus, while the mapped upper portion of the Shelf Projection blind fault (**Fig. 2**) may be inactive, the fault projects deeper beneath large anticlinoria and may be active at depth.

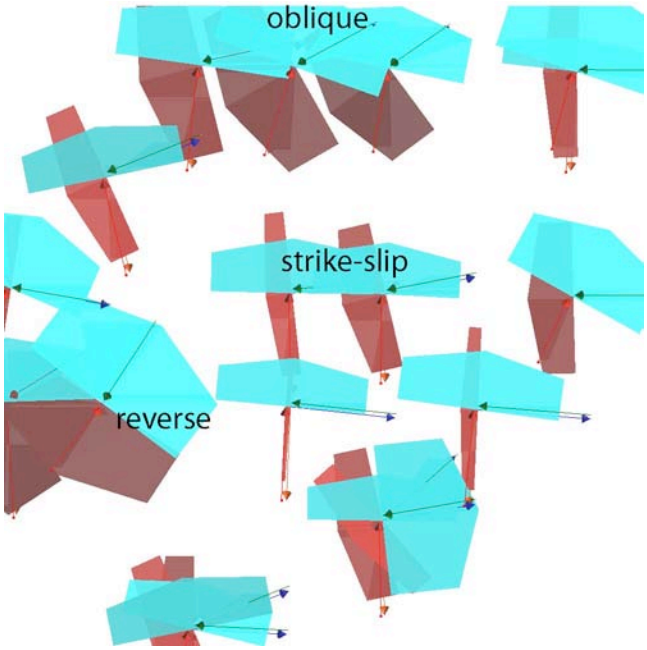

Figure 8: Our representation of earthquake nodal planes and slip using GOCAD. This view is straight down, with north to the top, and is of the Northridge aftershock zone. The chosen slip plane is red, the auxiliary plane is blue. Slip is shown for each side of each nodal plane. Several strike-slip mechanisms are shown in the center, a thrust is labeled, and oblique slip mechanisms are at the top.

We mapped a moderately NE-dipping fault near the base of the San Pedro escarpment in the hanging wall of the Shelf Projection blind fault (**Figs. 2, 10**). Faults along this trend have been called the San Pedro Escarpment fault zone (Nardin and Henyey, 1978; Bohannon et al., in press). Although we disagree with Bonannon et al. (in press) on the dip direction and sense of slip of the escarpment-forming fault zone, we retain the existing name. It is important to note that this fault extends along strike in both directions beyond where mapped, and so it is a larger earthquake source than what is shown in **Figure 2**. The strand of the San Pedro Escarpment fault that we mapped is the southwest edge of a narrow zone of faults. It dips northeast between 30° and 40°and thus converges downdip with the 20°-dipping Shelf Projection blind fault; they likely intersect at depth. Like the Dume segment of the Santa Monica fault (**Fig. 9a**), the San Pedro Escarpment fault may "cut off" slip on the deep fault, and may be an (oblique?) out-of-sequence thrust.

We cannot at this time tell whether the mapped strand of the San Pedro Escarpment fault flattens into the 20° dipping Shelf Projection blind fault, or if it continues at its 30° to 40° dip. Either

way, both faults project downdip close enough to the Compton-Los Alamitos thrust ramp of Shaw and Suppe (1996; Plesch and Shaw, 2002) that they may be the updip part of that fault. This is especially possible given that the depth of the Compton ramp may be unconstrained in this area and its dip is based on a model.

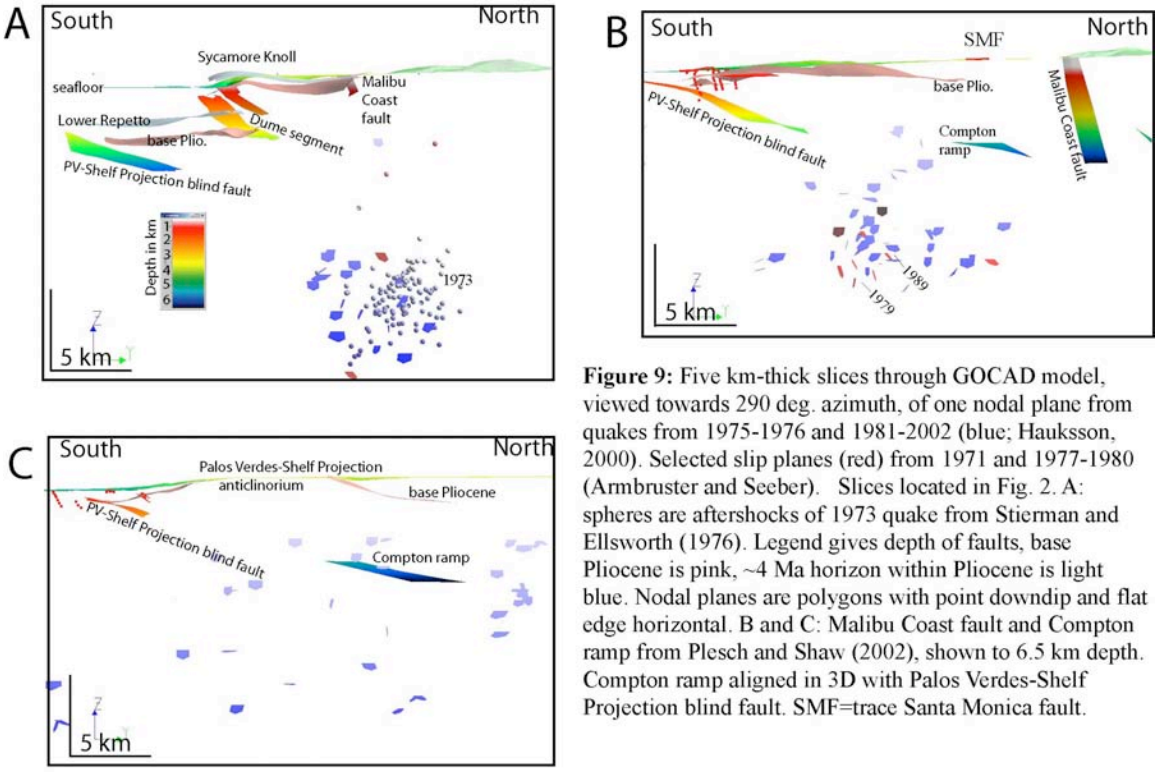

Figure 9: Five km-thick slices through GOCAD model, viewed towards 290 deg. azimuth, of one nodal plane from quakes from 1975-1976 and 1981-2002 (blue; Hauksson, 2000). Selected slip planes (red) from 1971 and 1977-1980 (Armbruster and Seeber). Slices located in Fig. 2. A: spheres are aftershocks of 1973 quake from Stierman and Ellsworth (1976). Legend gives depth of faults, base Pliocene is pink, ~4 Ma horizon within Pliocene is light blue. Nodal planes are polygons with point downdip and flat edge horizontal. B and C: Malibu Coast fault and Compton ramp from Plesch and Shaw (2002), shown to 6.5 km depth. Compton ramp aligned in 3D with Palos Verdes-Shelf Projection blind fault. SMF=trace Santa Monica fault.

The M5.0 1979 and 1989 earthquakes are spatially associated with the offshore part of the Palos Verdes-Shelf Projection anticlinorium. If the 20° dip of the Shelf Projection blind fault is projected into the Compton ramp as given by the CFM, these quakes, their aftershocks, and many other small quakes are beneath the fault (**Fig. 9**). If the variable 30° to 40° northeast dip of the San Pedro Escarpment fault strand is projected, the M5 quakes are beneath the fault but other quakes are near the fault. These quakes may be along and above a NE-dipping Miocene normal-separation fault whose seafloor trace is located farther to the southwest; we have little data across this fault and did not map it (**Figs. 4, 6**, see Larson, 2000). Relocated focal mechanisms of Hauksson (2000) and of Armbruster and Seeber do not show well-defined simple fault surfaces, although we have not focused our effort on interpreting the seismicity.

Basin Inversion and Basin Subsidence

Our new interpretation of the base Pliocene shows that the late Miocene section present in the hanging-wall of the Dume segment is not present in the footwall south of that fault. An angular unconformity separates the Pliocene strata from middle Miocene or older rocks. The regional and planar nature of this unconformity leads to the hypothesis that it was formed by wave erosion, and that beneath Hueneme Fan it has subsided as much as 4 km since the beginning of Pliocene time. This unconformity is time transgressive, as early Pliocene strata onlap or downlap onto it. The unconformity is as shallow as 1.5 km south of Point Dume. This does not necessarily mean a

much slower subsidence rate, because initiation of subsidence was delayed in that area. The top "Repetto" horizon downlaps onto it, and farther south, aggradation did not commence until after 2.5 Ma. Therefore, even though total subsidence is much greater beneath Hueneme Fan than south of Point Dume, subsidence rates may be similar. Early Pliocene "Repetto" strata are present offshore Venice Beach (see also Wright, 1991), and long-term average subsidence rates in that area are half those at Hueneme Fan.

DISCUSSION

Folds and the Fault Slips that Create Them

The Shelf Projection anticlinorium had previously been interpreted as en-echelon with, and distinct from, the Palos Verdes anticlinorium (Nardin and Henyey, 1978; Legg et al., in press). We remapped these anticlinoria and show that they are now a single structure, although with a slight local bend or right step in the axis (**Fig. 1**). We did not study the broad shelf south and southeast of Palos Verdes Hills; it is possible, perhaps likely, that the anticlinorium continues to the southeast. The studied 40+ km-long section of the anticlinorium, on both Palos Verdes Peninsula and at the Shelf Projection, include short-wavelength (1/2-1 km) folds. (**Fig. 10**; Dibblee, 1999; Fisher et al., 2003;). It is these folds that are en-echelon. The rocks involved in the short-wavelength folding are late Miocene (e.g., Nardin and Henyey, 1978), and we hypothesize that this short-wavelength folding occurred during (early?) Pliocene time and predates the larger structure. This folding succession may be common, as dated strata show that

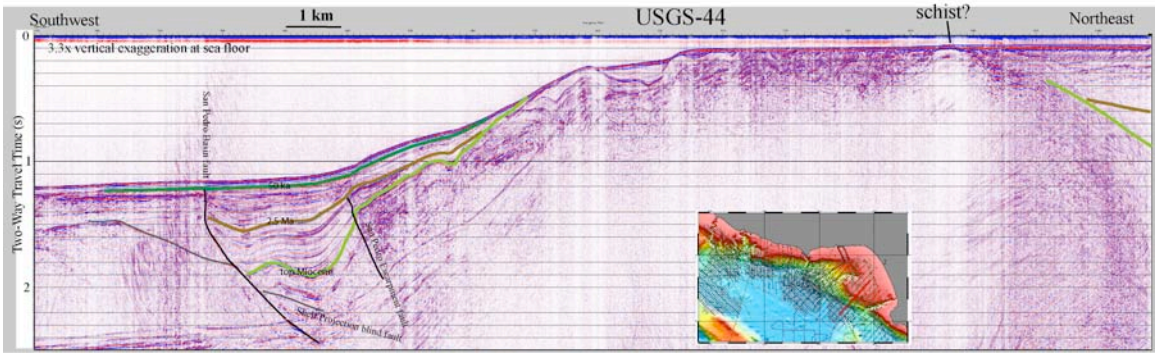

Figure 10A: Migrated stack of USGS 44, displayed in travel time, located as red line in inset and on Fig. 3A. Low-angle NE-dipping fault is the same as the one shown in Fig. 6. The San Pedro Basin fault likely offsets the low-angle fault. The part to the northeast was mapped as the Shelf Projection blind fault. Post-50 ka strata, above dark green, can be traced up the fold limb, and may be kinked above the tip of the San Pedro Escarpment fault. Top "Repetto" is brown; top Miocene is light green.

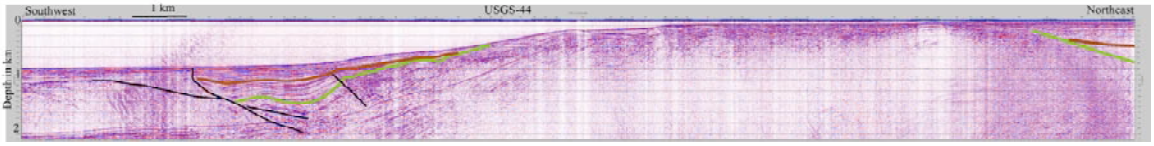

Figure 10B: Migrated stack of USGS 44, displayed in depth with no vertical exaggeration. This depth section was used for the top "Repetto" (brown) area balance shown in Figure 11A, B.

short-wavelength Pliocene folds precede long wavelength folding of the Channel Islands anticlinorium (Seeber and Sorlien, 2000).

Folds, in the absence of diapirism, are the product of slip on faults. If contraction is being actively absorbed in an anticline, then there must be a fault or ductile shear zone at depth that is

slipping. Broad fold limbs along the California margin have generally been described as backlimbs above ramps in faults, whether the fault ramp is planar above a kink, or curved in cross section (listric) (Davis and Namson, 1994a,b; Shaw and Suppe, 1994, 1996; Seeber and Sorlien, 2000). Where a broad, long anticlinorium has two limbs, one might expect one limb to be a forelimb, and the other to be a backlimb. The forelimb can be due to slip dying out (e.g., Wickham, 1995), or due to flattening of a fault at the top of a ramp (e.g., Suppe, 1983), or to both. However, in the cases of the Northern Channel Islands anticlinorium and also Palos Verdes anticlinorium, both fold limbs have been interpreted as backlimbs. The north or northeast limb has been explained as a backlimb above the fault that forms the base of a tectonic wedge, and the south or southwest limb has been explained as a second backlimb above a backthrust that forms the roof of the thrust wedge (Davis et al, 1989; Shaw and Suppe, 1994, 1996). However, in both areas faults are imaged that dip north and northeast respectively beneath the south and southwest-dipping fold limbs (**Figs. 4, 6, 10**, Sorlien et al., 2000). We prefer to interpret these fold limbs as forelimbs, and present a model for formation of broad forelimbs.

Many examples and publications include forelimbs that are narrower and more steeply dipping than the backlimb (Suppe, 1983; Suppe and Medwedeff, 1990). However, broad forelimbs can form independently of a backlimb. If the deep part of a planar fault is slipping, and the shallow part is not, a forelimb of an anticline will form (e.g., Sibson, 1985). If the fault is very broad and gently dipping, and the slip is absorbed gradually up the dip of the fault, the fold limb may be broad and gently dipping. A class of forelimbs has been quantified as trishear folds (Erslev, 1991; Hardy and Ford, 1997; Allmendinger and Shaw, 2000). They can explain progressively-tilting forelimbs, and involve a triangular shear zone above the tip of a propagating blind thrust. Line lengths and volumes need not be preserved, as material can be transferred between the hanging-wall and footwall sides or vice-versa of a shear zone as it propagates through the material. While we are investigating application of a trishear model to the Palos Verdes-Shelf Projection anticlinorium, here we will use a simple graphical approach and simple area balancing in cross section to estimate slip on the blind faults. In **Figure 11C-D**, we show a model where a gently-dipping, progressively tilting forelimb is created to absorb slip.

Slip Estimates

Figure 11A and **11B** shows two end-member area balances of the anticlinorium using the depth section of USGS-44 (**Fig. 10B**). The area balance is based on folding since the time of deposition of the top "Repetto", at approximately 2.5 Ma. Post-"Repetto" slip is modeled between 0.8 km or 1.7 km, depending on choice of fault dip and initial stratal dip. Area balance is a simple technique, where one calculates the excess area above an originally flat surface or regional dipping surface (Woodward et al., 1989; Epard and Groshong, 1993). This is usually done on a fold where the fault flattens into a regional decollement/detachment, and it is necessary to estimate the depth to that detachment. The slip is estimated by constructing a rectangle of equivalent area to that in the fold, with the base of the rectangle being at the depth to detachment, and its width being fault slip. Here, we do not use the depth to detachment, which might be at the

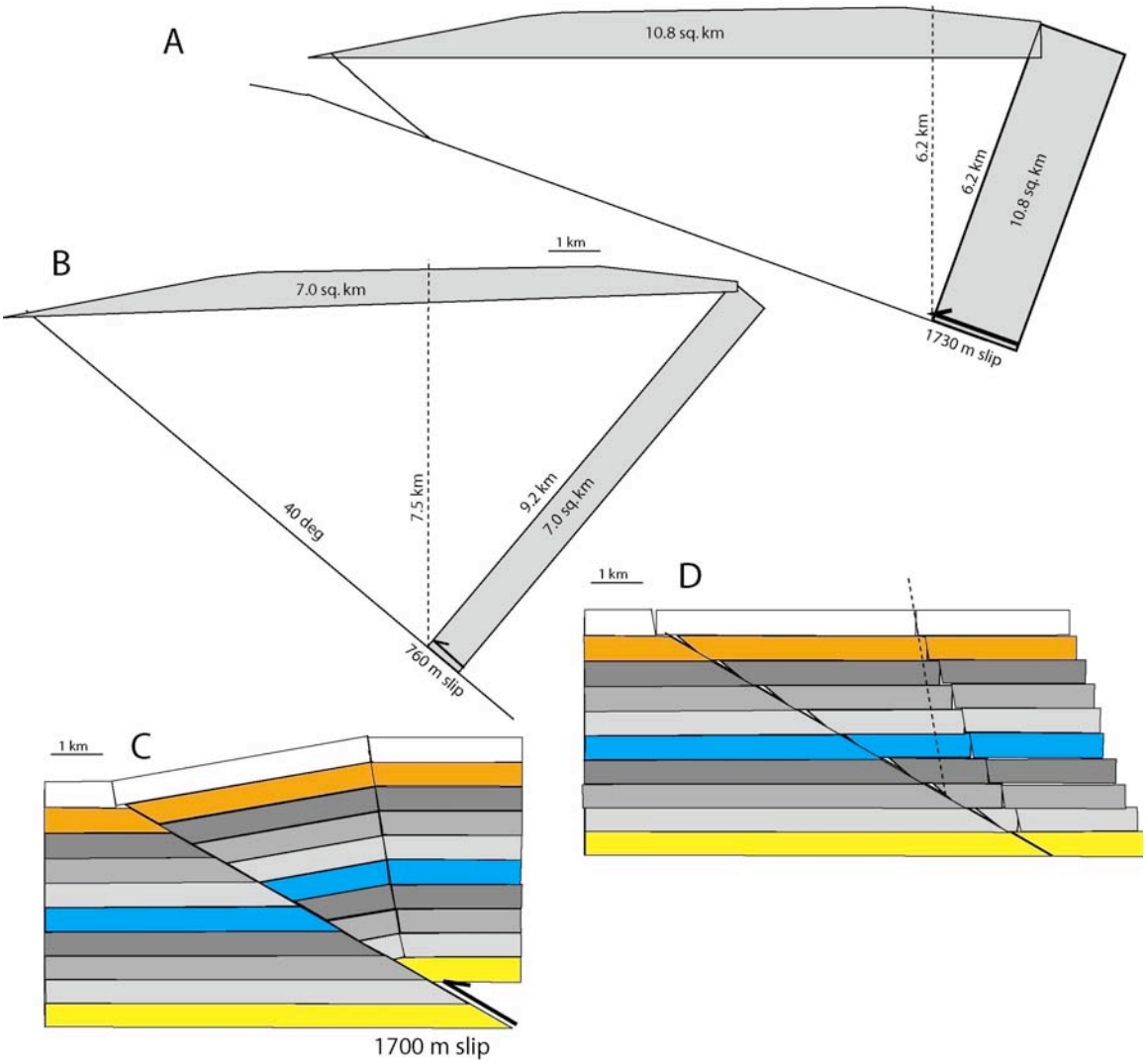

Figure 11: A: maximum slip area balance of USGS 44, resulting in an estimate of 1.7 km of slip in the last ~2.5 M.Y. A 20° dip is used for the Shelf Projection blind fault, and the area is based on zero initial dip. B: Minimum slip area balance, resulting in an estimate of 0.8 km of slip. A 40° dip for the San Pedro Escarpment fault is used, and the cross-sectional area of the fold is less because a 2° initial dip is assumed. C: Forelimb model for a fault where slip is gradually converted to folding by horizontal axis rotation of a triangular region. D: Restoration of the model in C, showing that bedding-parallel slip is expected and that the hinge must rotate or migrate through the material. Slip is 1.7 km for a 5 km-wide fold forelimb dipping 10°. This is the same slip estimate as the structural relief divided by the sin of the fault dip. This model is not intended to show the geometry imaged on USGS-44 (Fig. 10), but instead shows that broad, gently-dipping fold limbs can be interpreted as forelimbs, and that forelimbs need not be directly related to backlimbs. The strata are pre-thrust; syn-thrust strata would show progressive tilt and thinning in the hanging-wall.

base of the Compton thrust ramp of Shaw and Suppe (1996). Instead, the fold is interpreted as independent of the modeled kink at the base of the Compton ramp (Shaw and Suppe, 1996), and as being primarily a forelimb caused by slip dying out upwards. We balance the fold area with a sloping rectangle at the point where slip starts to be absorbed in the fold. As with the standard

application of area balancing, the rectangle is drawn with its long axis perpendicular to the direction of motion of the hanging-wall with respect to the footwall. Area balancing assumes that material does not move out of the plane of the section. In the case shown here, the right-lateral faults are northeast and southwest of the block being balanced, and do not affect the balance. The fold is long and continuous enough that minor strike-slip motion should not greatly affect the area balance.

An even simpler approach to estimating slip on blind or partially blind faults is to use trigonometry, fault dip, and structural relief, assuming simple block uplift of the hanging-wall. This was done to estimate Holocene slip on the Puente Hills thrust (Dolan et al., 2003). The same approach can be taken here: for a profile that has 0.85 km of structural relief due to slip on a fault dipping 30°, the slip is 1.7 km (**Fig. 11c**).

Figure 11A is the maximum slip estimate, where the Shelf Projection blind fault is aligned with the Compton thrust ramp along a 20 deg dip, and it is assumed that there is zero initial dip of the top Repetto. Slip is 1.7 km in this model. **Figure 11B** shows a minimum slip model. The shallow San Pedro escarpment fault dips about 40° near USGS44, but flattens to 30 deg and less at the NW and SE ends of its mapped portion (measured in GOCAD). The 40° dip is shown, and the area of the fold is smaller because an initial dip of 2° is assumed. There is less than 0.8 km of slip in the last 2.5 M.Y. in this model. Both models underestimate slip because volume is lost by sediment compaction and pressure solution. Other variables that are difficult to quantify are the initial dip and age of the top ”Repetto”. These slip estimates only apply to the part of the fault where the cross section is located.

In **Figures 11C** and **11D**, we show a model for creation of a forelimb by horizontal axis rotation. This model has similarities to the trishear model (Erslev, 1991; Hardy and Ford, 1997, Allmendinger and Shaw, 2000). It is also similar to a model for vertical axis rotations applied to the San Andreas fault system in Salton Trough, California (Armbruster et al., 1998). There, crustal slats of unequal lengths carry different amounts of plate motion for a given amount of rotation. The plate motion accommodated by clockwise rotation is not available for right-lateral motion on the bounding faults. Therefore, slip on the bounding faults is smallest adjacent to the longest rectangular block. Dextral shear is transformed gradually between clockwise rotation and right-lateral slip across triangular regions of rotating blocks bounded by NE-SE left-lateral faults (Armbruster et al. 1998). If **Figure 11C** was a map and not a cross section, left-lateral slip would be dissipated into counterclockwise slip of rectangular blocks separated by right-lateral faults. For **Figure 11C** viewed as a cross section, thrust slip is dissipated into forelimb rotation, with bedding-parallel slip. The fault continues to slip adjacent to the tilting forelimb, rather than folding occurring above the tip of a propagating fault. Many of the faults in the study area are reactivated Miocene normal-separation faults, so that propagation of a new fault need not occur. The model shown has a 5 km-wide limb dipping 10 deg, which is the same as the limb constructed on the top “Repetto” on USGS44 (**Fig. 10B**). Slip is 1.7 km. This is an overestimate if some of the structural relief is due to initial dip. This model is not equivalent to the actual geometry seen on USGS-44 because it does not include the progressive tilting that occurred between 5 and 2.5 Ma, and because a clearly triangular fold limb has not been imaged. As discussed in papers on the Trishear model, propagation of the tip of the blind fault, motion of material through the triangular deformation zone, or curved rather than kinked fold limbs are

possible or likely. However, the 1.7 km slip estimate should be accurate because it is the same as structural relief divided by sin(fault dip).

Palos Verdes Peninsula has active surface and rock uplift (LaJoie, 1986). This uplift has been explained as the result of ~3 mm/yr right-lateral slip on the Palos Verdes fault, and a restraining segment (Ward and Valensise, 1994). While the restraining segment supplies a component of convergence, this convergence need not be accommodated solely on the Palos Verdes fault. The width of the fold suggests involvement of a low-angle fault (e.g., Shaw and Suppe, 1996). Ward and Valensise (1994) only explained uplift with respect to sea-level. Based partly on paleo-bathymetry estimates based on paleontology, the increase of structural relief was considered the result of uplift from an initial depth of 850 m (Ward and Valensise, 1994). The Quaternary uplift rate is obtained from elevations of coastal terraces and their inferred ages (Ward and Valensise, 1994). This uplift with respect to sea level underestimates increase in structural relief if Santa Monica and San Pedro basins are subsiding (Bohannon et al., in press; see Pinter et al., 2003)

Figures 4, 6, and 10 show that the present bathymetric basin lies above the footwall of a zone of NE-dipping faults inferred to have been normal faults during the Miocene. The thin post-Miocene strata above this footwall are consistent with it having been higher-standing than the hanging-wall (includes Palos Verdes Hills). It is expected that growth of the Palos Verdes-Shelf Projection anticlinorium would result in an isostatic response contributing to subsidence of the San Pedro basin. If structural relief is increasing faster than the surface uplift of Palos Verdes Hills, then slip on the San Pedro Escarpment fault or another blind fault is needed to make up the difference.

We have calculated long-term average slip rates of blind faults beneath the Shelf Projection, and now discuss evidence for post-50 ka activity. It is published that folding in this area predates 1 Ma, probably because shallow reflections appear to onlap the fold without being involved in the folding (Nardin and Henyey, 1978). Our reprocessing of USGS data attenuated multiples and images progressively-tilted Pliocene strata on the north limb of the fold (**Fig. 5**). Rapid (.28-.58 mm/yr) Holocene sedimentation shown in cores (Sommerfield and Lee, 2003), and an unconformity imaged at ~300 m below sea floor on certain seismic-reflection profiles, suggests that the non-tilted strata are younger than 0.5 to 1.0 million years, or younger if sedimentation rates have been higher during glacial periods. In addition, lack of northeast limb tilting does not preclude blind fault slip being absorbed in the southwest limb (Fig. 11C). The Miocene strata beneath the Shelf Projection are not deeply eroded, so we cannot call upon rapid rock uplift in this area. However, the wavecut platform cut into Miocene rocks on the Shelf Projection is shallower than eustatic sea level lowstands, suggesting some ongoing rock uplift. If the footwalls of the thrust faults are subsiding, then structural relief is growing faster than rock uplift (Pinter et al., 2003). However, we do not have direct evidence for or against ongoing footwall subsidence in this area.

Post-50 ka strata provide more direct evidence for ongoing deformation. A reflection from the base of ODP site 1015 was correlated to the southwest limb of the anticlinorium (Shipboard Scientific Party, 1997; Piper, et al., 2003). Post-50 ka strata can be followed about 300 vertical meters up the south fold limb on several profiles (**Fig. 10**). Most of this relief is in the hanging-wall of the mapped strand of the San Pedro Escarpment fault zone. Ascribing this relief to

folding results in impossibly high estimates of slip. Therefore, these strata must "drape" the fold limb; having been deposited with an initial dip as high as 8°. Turbidity currents can deposit sediment as much as 100 m above the basin floor, with thinning and fining of sediment along the basin margins (ongoing research by W. Normark). An unknown part of the remaining 200 m of relief could be due to active tilting of the southwest limb.

The Palos Verdes-Shelf Projection anticlinorium may have propagated northwest across Santa Monica Canyon. Gardner et al. (2003) show NE-SW cross-sections across the slope north of Santa Monica Canyon. These cross sections show a convex-up seafloor where concave-up might be expected ("convex-up" label in **Fig. 3B**). They ascribe this to a depocenter (Gardner et al. 2003). Two piston cores taken at this seafloor bulge show the strata to be 14,560-15330 and 7910-8130 calibrated years B.P. (Sommerfield et al., 2003). Seismic reflection profiles do not support the depocenter interpretation. However, the few profiles in this area available to us do not clearly show whether or not the Holocene strata are folded or just draped across deeper structure. However, Santa Monica Canyon is more deeply entrenched in the area of this seafloor bulge, suggesting folding (**Fig. 3B**).

The possibility of drape of Holocene and post-50 ka strata has made it very difficult for us to use these strata to provide estimates of rates of ongoing folding. This drape also calls into question slip estimates elsewhere around Los Angeles basin that are based on dips or structural relief of turbidites. Clearly, this is an area for focused sedimentologic study.

CONCLUSIONS

Digital maps were provided to the SCEC Community Fault Model of several faults. These maps include the offshore Malibu Coast fault, linking faults between the Dume segment of the Santa Monica fault and the Malibu Coast fault, and part of the offshore Santa Monica fault. Structure-contour maps were constructed of the base Pliocene and a ~2.5 Ma horizon. The base of ~50 ka strata was correlated from ODP site 1015 to several faults and folds. The Palos Verdes anticlinorium extends 25+ km west-northwest into Santa Monica Bay, beneath the Shelf Projection. The offshore part includes a progressively-tilting north limb, and a broad south limb. Northeast-dipping blind faults project beneath this structure and close to the Compton thrust ramp. The scale of the active Palos Verdes-Shelf Projection anticlinorium suggests a minimum 800 square km underlying fault-and we have not included possible offshore continuations south of Palos Verdes Hills and an area of convex-up seafloor north of Santa Monica Canyon.

Broad fold limbs have generally been modeled as backlimbs above thrust ramps, or backlimbs above the top of thrust wedges, with the interpreted fault dipping the same direction as the fold limb dip in both cases. Here, we present a model that can explain broad, gently-dipping forelimbs, where the fault dips and limb dip are opposite. This model and area balancing in cross-section were used to estimate slip on blind faults beneath the Shelf Projection. Dip-slip on blind faults beneath this part of the anticlinorium is as much as 1.7 km in the last 2.5 M.Y., or more if sediment compaction and pressure solution are significant. We infer that these blind faults are still active. Although post-50 ka strata are present on the southwest fold limb, we were not able to estimate a rate of folding based on them. That is because thick turbidite flows result in drape of the flanks of the basin. The base of the post-50 ka strata has 40 m of relief across the

right-lateral San Pedro Basin fault, part by faulting and the remainder by folding and possibly drape.

Acknowledgements

Drew Mayerson and others at the U.S. Minerals Management Service provided access to the Digicon data, Tom Wright's and David Okaya's efforts made Exxon data available to SCEC researchers, other industry sources provided additional data. John Armbruster did one set of the earthquake relocations. Egill Hauksson provided a more up-to-date version of the relocated hypocenters referenced as Hauksson (2000). Bruce Luyendyk is supervising Kris Broderick's thesis. Information on petroleum wells along the Los Angeles area coast was found in the repository at Long Beach State operated by Dan Francis. Discussions with Bob Bohannon and Shirley Baher of USGS are appreciated. Eight meter horizontal resolution Multibeam data were provided by P. Dartnell.

Note: We have in past abstracts and reports changed the name that we call the Shelf Projection Blind fault. Both the eastern Shelf Projection Blind fault and the San Pedro Escarpment fault may be updip splays of the Compton-Los Alamitos blind thrust. If this relation can be shown with a high degree of confidence, then a single name for all parts of this fault will be less confusing.

REFERENCES

Allmendinger, R. W., and Shaw, J. H., 2000, Estimation of fault propagation distance from fold shape: Implications for earthquake hazard assessment, Geology, v. 28, p. 1099-1102.

Armbruster, J. G., Seeber, L., Sorlien, C. C., and Steckler, M. S., 1998, Rotation vs rifting in an extensional jog: Salton trough, California, EOS, (Trans. AGU), v. 79, no. 45, p. F565.

Blake, G. H., 1991, Review of the Neogene biostratigraphy and stratigraphy of the Los Angeles Basin and implications for basin evolution, in *Active Margin Basins*, K.T. Biddle (Editor), AAPG Memoir **52**, 135-184.

Bohannon, R. G., Gardner, J. V., and Sliter, R. W., in press, Holocene to Pliocene Tectonic Evolution of the Region Offshore of the Los Angeles Urban Corridor, Southern California, Tectonics.

Burdick, D. J., and Richmond, W. C., 1982, A summary of geologic hazards for proposed OCS oil and gas lease sale 68, Southern California, MMS and USGS Open-File Report 82-33.

California Division Oil, Gas, and Geothermal Resources, 1992, California Oil & Gas Fields, Volume II: Southern, Central Coastal, and Offshore California, Pub. TR11.

Davis, T. L., and Namson, J. S., 2000, An evaluation of the subsurface structure of the Playa Vista Project Site and Adjacent area, Draft Environmental Impact Report (DEIR), Village at Playa Vista, vol. 5, Technical Appendix D-4, "Earth", 2003, Appendix D-4: City of Los Angeles/EIR No. ENV-2002-6129-EIR State Clearinghouse no. 2002111065.

Davis, T. L., Namson, J., and Yerkes, R. F., 1989, A cross section of the Los Angeles Area: Seismically active fold and thrust belt, the 1987 Whittier Narrows earthquake, and earthquake hazard, Journal of Geophysical Research, vol. 94, no. B7, p. 9644-9664.

Davis, T. L., and Namson, J. S., 1994a, A balanced cross-section of the 1994 Northridge earthquake, southern California, Nature, vol. 372 p. 167-169.

Davis, T. L., and Namson, J., 1994b, Structural analysis and seismic potential evaluation of the Santa Monica Mountains anticlinorium and Elysian Park thrust system of the Los Angeles basin and Santa Monica Bay, National Earthquake Hazard Reduction Program Award #1434-93-G-2292.

Dartnell, P., and J. V. Gardner, 1999, Sea-Floor Images and Data from Multibeam Surveys in S.an Francisco Bay, Southern California, Hawaii, the Gulf of Mexico, and Lake Tahoe, California-Nevada, *U.S. Geol. Surv. Digital Data Series* DDS-55 Version 1.0.

Dibblee, T. Jr., 1999, Geologic map of Palos Verdes Peninsula and Vicinity, Redondo Beach, Torrance, and San Pedro Quads, LA County, CA ed. H. E. Ehrenspeck, P.L. Ehlig, and W. L. Bartlett, Dibblee Foundation, Santa Barbara, 1:24,000.

Dolan, J. F., Christofferson, S. A., and Shaw, J. H., Recognition of paleoearthquakes on the Puente Hills blind thrust fault, California, Science, v. 300, p. 115-118.

Epard, J.-L., and Groshong, R. H., 1993, Excess Area and Depth to Detachment, American Association of Petroleum Geologists Bulletin, v. 77, p. 1291-1302.

Erslev, E. A., 1991, Trishear fault-propagation folding, Geology 19, p. 617-620.

Fisher, M. A., W. R. Normark, R. G. Bohannon, R. W. Sliter, and A. J. Calvert, 2003, Geology of the continental margin beneath Santa Monica Bay, southern California, from seismic reflection data, *Bull. Seism. Soc. Amer., v.* 93 p. 1955-1983.

Gardner, J. V., Dartnell, P., Mayer, L. A., and Clarke, J. H., 2003, Geomorphology, acoustic backscatter, and processes in Santa Monica Bay from multibeam mapping, Marine Environmental Research, v. 56, p. 15-46.

Hardy, S., and Ford, M., 1997, Numerical modeling of trishear fault propagation folidng, Tectonics, v. 16, no. 5, p. 841-854.

Hauksson, E. and G. V. Saldivar (1986). The 1930 Santa Monica and the 1979 Malibu, California, earthquakes, *Bull. Seism. Soc. Amer.* 76, p. 1542-1559.

Hauksson, E., 1990, Earthquakes, faulting, and stress in the Los Angeles Basin, *J. Geophys. Res.* **95**, 15365-15394.

Hauksson, E., 2000, Crustal structure and seismicity distribution adjacent to the Pacific and North America plate boundary in southern California, J. Geophys. Res., 105, 13,875-13,903.

Kamerling, M. J., and Luyendyk, B.P., 1979, Tectonic rotations of the Santa Monica Mountains region western Transverse Ranges, California, suggested by paleomagnetic vectors, Geological Society of America Bulletin, Part 1, vol. 90, p. 331-337.

Lajoie,K.R., 1986, Coastal tectonics, in R. E. Wallace, ed., Active Tectonics, National Academy Press, Washington, D. C., p. 95-124.

Larson, A. A., 2000, Defining the fault that caused the 1979 and 1989 Malibu Earthquakes (M 5.0) in Santa Monica Bay, California, Senior Thesis, Department Earth and Planetary Sciences, Harvard University, Cambridge, Massachusetts, 65 pages.

Legg, M. R., M. J. Kamerling, and R. D. Francis, 2004, Termination of strike-slip faults at convergence zones within continental transform boundaries: Examples from the California Continental Borderland, in Grocott, J., McCaffrey, K., Taylor, G., and Tikoff, B., eds., Vertical Coupling and Decoupling in the Lithosphere: Geological Society of London Special Publication, (in press).

Mallet, J. L., 1992, Discrete smooth interpolation in geometric modeling, Computer Aided Design, 24, 178-191.

Mallet, J. L., 1997, Discrete modeling for natural objects, Mathematical Geology, 29, 199-219.

Normark, W. R., and McGann, M., 2003, Developing a high resolution stratigraphic framework for estimating age of fault movement and landslides in the California Continental Borderland, SCEC Annual Meeting abstracts, v.13, p. 121-122.

Nardin, T. R., and T. L. Henyey, 1978, Pliocene-Pleistocene diastrophism of Santa Monica and San Pedro shelves, California Continental Borderland, *Amer. Assoc. Petroleum Geol. Bull.* **62**, 247-272.

Pinter, N., Sorlien, C. C., and Scott, A. T., 2003, Fault-related fold growth and isostatic subsidence, California Channel Islands, American Journal of Science, v. 303, p. 300-318.

Piper, D. J. W., Normark, W. R., and McGann, M., 2003, Variations in accumulation rate of late Quaternary turbidite deposits in Santa Monica Basin, offshore southern California: Eos Trans. AGU, 84(46), Fall Meet. Suppl., Abstract OS52B-0916.

Plesch, A., and Shaw, J. H., 2002, SCEC 3D Community fault model for southern California, Eos Trans. AGU, 83 (47), Fall Meeting Suppl., Abstract S21A-0966, and http://structure.harvard.edu/cfma (includes Broderick, Kamerling and Sorlien maps).

Seeber, L, and Sorlien, C. C., 2000, Listric thrusts in the western Transverse Ranges, California, Geological Society of America Bulletin, v. 112, p. 1067-1079.

Shaw, J. H., and Suppe, J., 1994, Active faulting and growth folding in the eastern Santa Barbara Channel, California, Geological Society of America Bulletin, vol. 106, p. 607-626.

Shaw, J. H., and J. Suppe (1996). Earthquake hazards of active blind-thrust faults under the central Los Angeles basin, California, *J. Geophys. Res.* **101**, 8623-8642.

Shipboard Scientific Party, 1997, 9. Site 1015, in *Proceedings of the Ocean Drilling Program, Initial Reports* **167**, M. Lyle, I. Koizumi, I., and C. Richter, (Editors), 223-237.

Sibson, R. H., 1995, Selective fault reactivation during basin inversion: Potential for fluid redistribution through fault-valve action, from Buchanan, J. G., and Buchanan, P. G., (eds.), Basin Inversion, Geological Society Special Publication no. 88, p. 3-19.

Sommerfield, C. K., and Lee, H., 2003, Magnitude and variability of Holocene sediment accumulation in Santa Monica Bay, California, Marine Environmental Research 56 p. 151-176.

Sorlien, C. C., Kamerling, M. J., Broderick, K., and L. Seeber, 2003, Structure and kinematics along the thrust front of the Transverse Ranges: 3D digital mapping of active faults in Santa Monica Bay using reflection, well, and earthquake data: Collaborative research with University of California, Santa Barbara, and Columbia University, Final Technical Report to U. S. Geological Survey NEHRP 02HQGR0013, 15 pages.

Sorlien, C. C., Pinter, N, Kamerling, M. J., and Scott, A. T., 2000, Late Quaternary Coastal Terraces and Lowstand Deltas Record Southward Migration of the Northern Channel Islands Anticline, California, EOS, (Trans. AGU), v. 81, p. F1169.

Stierman, D. J., and Ellsworth, W. L., 1976, Aftershocks of the February 21, 1973 Point Mugu, California earthquake, Bulletin of the Seismological Society of America, vol. 66, no. 6, p. 1931-1952.

Suppe, J., 1983, Geometry and kinematics of fault-bend folding, American Journal of Science, vol. 283, p. 684-721.

Suppe, J., and Medwedeff, D. A., 1990, Geometry and kinematics of fault-propagation folding, Eclogae geol. Helv. 83/3 p. 409-454.

U. S. Geological Survey and Southern California Earthquake Center, Scientists of, 1994, The magnitude 6.7 Northridge, California earthquake of 17 January, 1994, Science 266, p. 389-397.

Vedder, J. G., 1990, Maps of California Continental Borderland showing compositions and ages of samples acquired between 1968 and 1979, U. S. Geological survey Miscellaneous Field studies Map, Map MF-2122.

Ward, S. N., and Valensise, G., 1994, The Palos Verdes terraces, California: Bathtub rings from a buried reverse fault, Journal of Geophysical Research, vol. 99, no. B3, p. 4485-4494.

Wickham, J., 1995, Fault displacement-gradient folds and the structure at Lost Hills, California (U.S.A.), Journal of Structural Geology, v. 191, p. 1293-1302.

Woodward, N. B., Boyer, S. E., and Suppe, J., 1989, Balanced geological cross-sections: An essential technique in geological research and exploration, American Geophysical Union Short Course in Geology: volume 6, Washington, D.C.

Wright, T.L., 1991, Structural geology and tectonic evolution in the Los Angeles Basin, California, in K.T. Biddle, ed., Active Margin Basins, AAPG Memoir 52, American Association of Petroleum Geologists, Tulsa, p.35-135.

Reports Published

An unpublished manuscript will be rewritten as two separate papers, one on the Santa Monica-Dume fault and another on the material discussed in this report. The Masters thesis of Kris Broderick, in preparation, will cover material similar to what is in this report; his graduate studies were partially supported by USGS-NEHRP.

Sorlien, C. C., Broderick, K., Kamerling, M. J., Fisher, M., Normark, W., Sliter, R., and Seeber, L, 2003a, Structure and kinematics beneath Santa Monica Bay, California, Pacific Section AAPG abstracts, May 2003, Long Beach

Sorlien, C. C., Broderick, K., Sliter, R., Fisher, M., Normark, W., Seeber, L., and Kamerling, M. J., 2003b, Contributions to the SCEC Community Fault Model: Relating onshore-offshore stratigraphy and fault-fold activity beneath Santa Monica Bay, Annual Report to Southern California Earthquake Center, USC.

Plus two abstracts at SCEC Annual Meeting, September 2003.

Paper supported by previous NEHRP grant.

Pinter, N., Sorlien, C. C., and Scott, A. T., 2003, Fault-related fold growth and isostatic subsidence, California Channel Islands, American Journal of Science, v. 303, p. 300-318

Data Availability

Well data, including sonic surveys, are public and available from the California Division of Oil and Gas in Long Beach, Dan Francis' data repository at Long Beach, or from us. Wells in Federal waters (more than 5 km from the coast) are usually available from the US Minerals Management Service in Camarillo, but the wells in Santa Monica Bay all predate 1970 and the MMS does not seem to have information on them. The 800x2500 m grids of single channel sparker data, minisparker, and 3.5 kHz data are described in Burdick and Richmond (1982), but are apparently are missing from the sets of microfilm available from the NGDC. The originals can be found with difficulty from the US Minerals Management Service, but it is probably simpler to contact us. A 2.5 km by 2.5 km grid of non-migrated mid-1970s-vintage multichannel seismic reflection data from Digicon has been released by the U.S. Minerals Management Service and the films are in Camarillo. A grid of migrated seismic reflection data from Exxon is available from the Southern California Earthquake Center (contact David Okaya). Other industry seismic reflection data used in this project are not available, but may become available as part of the ongoing effort to transcribe and make public industry data. Our digital structure-contour maps of faults have been provided to the SCEC Community Fault Model (CFM) (http://structure.harvard.edu/cfma/), although some of our faults are not in version CFM-1.01beta. The structure-contour maps of stratigraphic horizons will be made available either through SCEC-CFM or as supplemental data to publications. BASIC programs and awk scripts were written to convert focal mechanism data (e.g., Hauksson, 2000) into our GOCAD format. These are available from C. Sorlien, but are in an old version of Omikron BASIC and would have to be reprogrammed for other languages. Contact Christopher Sorlien at chris@crustal.ucsb.edu for additional information on data.